Catalytic Mechanism of Phosphorylase Kinase Probed by Mutational Studies[†,‡]

V. T. Skamnaki,[§,||] D. J. Owen,[§,⊥] M. E. M. Noble,[#] E. D. Lowe,[#] G. Lowe,[▽] N. G. Oikonomakos,[||] and L. N. Johnson*[,#]

Laboratory of Molecular Biophysics and Oxford Centre for Molecular Sciences, Department of Biochemistry, Rex Richards Building, South Parks Road, Oxford OX1 3QU, U.K., National Hellenic Research Foundation, Institute for Biological Research and Biotechnology, 48 vas Constantinou Avenue, Athens 116 35, Greece, MRC Laboratory of Molecular Biology, Hills Road, Cambridge, CB2 2QH, U.K., and Dyson Perrins Laboratory, University of Oxford, South Parks Road, Oxford OX1 3QY, U.K.

Received June 24, 1999; Revised Manuscript Received August 27, 1999

ABSTRACT: The contributions to catalysis of the conserved catalytic aspartate (Asp149) in the phosphorylase kinase catalytic subunit (PhK; residues 1−298) have been studied by kinetic and crystallographic methods. Kinetic studies in solvents of different viscosity show that PhK, like cyclic AMP dependent protein kinase, exhibits a mechanism in which the chemical step of phosphoryl transfer is fast and the rate-limiting step is release of the products, ADP and phosphoprotein, and possibly viscosity-dependent conformational changes. Site-directed mutagenesis of Asp149 to Ala and Asn resulted in enzymes with a small increase in K_m for glycogen phosphorylase b (GPb) and ATP substrates and dramatic decreases in k_{cat} (1.3×10^4 for Asp149Ala and 4.7×10^3 for Asp149Asn mutants, respectively). Viscosometric kinetic measurements with the Asp149Asn mutant showed a reduction in the rate-limiting step for release of products by 4.5×10^3 and a significant decrease (possibly as great as 2.2×10^3) in the rate constant characterizing the chemical step. The date combined with the crystallographic evidence for the ternary PhK-AMPPNP-peptide complex [Lowe et al. (1997) *EMBO J. 6*, 6646−6658] provide powerful support for the role of the carboxyl of Asp149 in binding and orientation of the substrate and in catalysis of phosphoryl transfer. The constitutively active subunit PhK has a glutamate (Glu182) residue in the activation segment, in place of a phosphorylatable serine, threonine, or tyrosine residue in other protein kinases that are activated by phosphorylation. Site-directed mutagenesis of Glu182 and other residues involved in a hydrogen bond network resulted in mutant proteins (Glu182Ser, Arg148Ala, and Tyr206Phe) with decreased catalytic efficiency (approximate average decrease in k_{cat}/K_m by 20-fold). The crystal structure of the mutant Glu182Ser at 2.6 Å resolution showed a phosphate dianion about 2.6 Å from the position previously occupied by the carboxylate of Glu182. There was no change in tertiary structure from the native protein, but the activation segment in the region C-terminal to residue 182 showed increased disorder, indicating that correct localization of the activation segment is necessary in order to recognize and present the protein substrate for catalysis.

Eukaryotic protein kinases catalyze the transfer of the ATP γ phosphate group to serine, threonine, or tyrosine residues on target proteins. In most protein kinases, the reaction is tightly controlled by additional subunits and by phosphorylation. Once activated, protein kinases catalyze phosphorylation of their specific targets resulting in enhancement or inhibition of biological activity in proteins involved in intracellular signaling pathways. The eukaryotic protein kinases represent one of the largest protein superfamilies. In the recently sequenced nematode *C. elegans* genome, there are 410 eukaryotic protein kinase domain genes (*1*) corresponding to about 2% of the total predicted protein coding genes. The estimate by Hunter (*2*) that there may be more than 1000 protein kinases in the mammalian genome still appears valid. Similarities in sequence indicated that all protein kinases share a common core of about 270 amino acids (*3*), and the notion of a common fold has been substantiated by crystal structures of at least 19 protein kinases (*4*). The structures of active kinases display a similar conformation in key regions involved in ATP and protein substrate recognition. The structures of inactive kinases show variations, especially in the relative orientations of the two lobes of the bilobal protein, in the regions of control loops and an α-helix that contributes residues to the ATP binding site, and in the disposition of individual residues within a common core.

Phosphorylase kinase, the first protein kinase to be discovered (*5*), catalyses the phosphorylation of a single serine residue, Ser14, thereby converting inactive phosphorylase b (GPb) to active glycogen phosphorylase a (GPa) and stimulating glycogen degradation. The enzyme integrates

[†] This work has been supported by the BBSRC, MRC, and EPSRC through the grant to the Oxford Centre for Molecular Sciences and the Wellcome Trust through a Collaborative Travel Award.

[‡] Coordinates have been deposited in the Protein Data Bank with accession number 1QL6.

* To whom correspondence should be addressed. Phone: 44-1865-275365. Fax: 44-1865-510454. E-mail: Louise@biop.ox.ac.uk.

[§] Joint first authors.

[||] Institute for Biological Research and Biotechnology.

[⊥] MRC Laboratory of Molecular Biology.

[#] Laboratory of Molecular Biophysics and Oxford Centre for Molecular Sciences.

[▽] Dyson Perrins Laboratory.

10.1021/bi991454f CCC: $18.00
Published on Web 10/14/1999

extracellular signals that arise from hormone receptor interactions and from neuronal impulses mediated through calcium, with those that arise from changes in concentrations of intracellular metabolites to provide a tightly controlled kinase activity (reviewed in ref *6*). Phosphorylase kinase is one of the largest of the protein kinases and is composed of four types of subunit, with stoichiometry $(\alpha\beta\gamma\delta)_4$ and a total molecular mass of 1.3×10^6 Da. The α and β subunits are regulatory and are the targets for control by phosphorylation by cyclic AMP dependent protein kinase (cAPK). The δ subunit is essentially identical to calmodulin and confers calcium sensitivity. The 386 residue γ subunit is the catalytic subunit that comprises an N-terminal catalytic region and a C-terminal calmodulin-binding region. The kinase domain of the γ subunit (here abbreviated as PhK)[1] comprising residues 1−298 has been expressed and crystallized and the crystal structure solved (*7*, *8*). The kinase domain is a fully active protein kinase that is constitutively active without the requirement for activation by phosphorylation or other effectors and provides a model system for the study of kinase catalysis and substrate recognition without the complications of posttranslational modification or control mechanisms.

In vivo, phosphorylase is the only recognized substrate of phosphorylase kinase, but in vitro, the enzyme will catalyze phosphorylation of a number of other proteins and peptide substrates with decreased efficiency compared with the natural substrate (*6*). Analysis of sequences surrounding the sites of phosphorylation indicate a consensus sequence of (R/K)XXS*(V/I)Z using the single letter amino acid code where S* is the serine phosphorylated and X and Z may be any amino acid, but activity is increased if Z is an arginine as in phosphorylase. Peptide substrates exhibit K_m values (about 1 mM) that are higher than the K_m values observed for phosphorylase (values range 44−270 μM for the holoenzyme; and 9−27 μM for the truncated γ subunit), suggesting that the phosphorylase molecule may make additional contributions to recognition and affinity in regions distinct from the immediate surroundings of the serine phosphorylated (*9*). Indeed only one of the 29 serines in phosphorylase is phosphorylated, although some other serines are surrounded by a consensus sequence motif. We have used a modified high-affinity peptide (sequence RQMS*FRL termed MC-peptide) to study the structure of the ternary PhK-AMPPNP-peptide complex (*10*).

With the exception of a plant putative protein kinase (*11*), all eukaryotic protein kinases contain a conserved aspartic acid (Asp149 in PhK) located in subdomain VIb as defined by Hanks and Hunter (*3*). Structural studies on three protein kinases in ternary complexes with ATP analogues and substrate peptides (cAPK, the insulin receptor tyrosine kinase, IRK, and PhK) (*10*, *12*−*15*) have shown that the aspartate is located in a position in which it is likely to participate in catalysis (Figure 1). At least three possibilities have been suggested for the role of the aspartate: (i) that it could function as a general base [as proposed in a mechanism described in (*16*)] to abstract a proton from the hydroxyl group of the serine, threonine, or tyrosine residue of the protein substrate, thereby promoting nucleophilic attack on the γ phosphate of ATP; (ii) that it functions as a hydrogen bond acceptor to facilitate phosphoryl transfer by promoting the correct orientation of the hydroxyl for attack on the γ phosphate of ATP and that the proton is delivered to solvent after phosphoryl transfer (*17*); (iii) that, in addition to its role in orientation, the aspartate enhances the reactivity of the γ phosphate of ATP toward electrophilic attack (*18*).

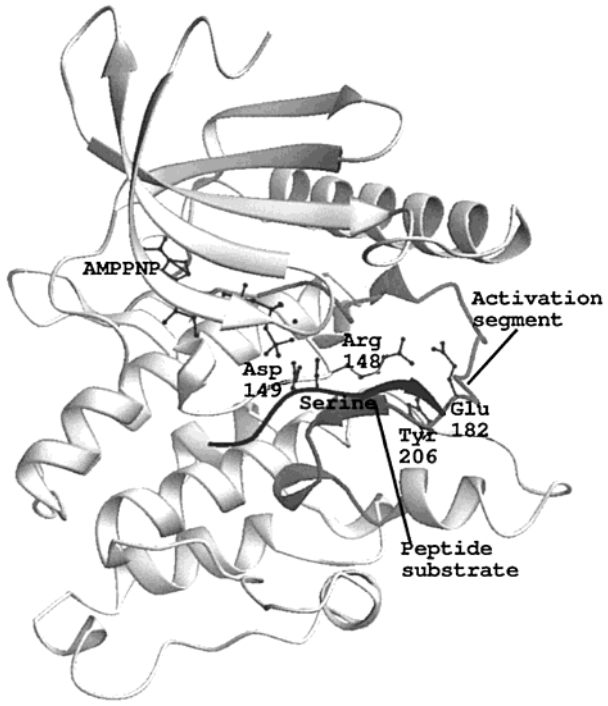

FIGURE 1: Schematic diagram of phosphorylase kinase (PhK) in ternary complex with AMPPNP/Mn^{2+} and MC-peptide substrate (*10*). The catalytic aspartate, Asp149, and Glu182 and contact residues from the activation segment are shown. The peptide substrate is indicated in black and the activation segment by dark gray. Diagram by OGLOBJECTS (M.E.M.N., unpublished material).

In cAPK, the kinase reaction proceeds with a fast chemical step in which the γ phosphate of ATP is transferred to the peptide substrate. This is followed by rate-limiting release of products (*19*). In cAPK the affinity of the phosphopeptide is less than that of ADP (*20*) and it is inferred that release of ADP represents the slowest step. Kinetic studies in which the burst phase in cAPK activity was monitored with rapid quench flow techniques have shown that the rate constant for this phase is independent of pH between pH 6 and 9 (*17*). Moreover, with a cAPK substrate peptide that lacked an arginine in the P-2 position, no pK_a of the acid limb of the pH profile of k_{cat}/K_m was observed, indicating that the group(s) of pK_a 6.2−6.4 observed in earlier kinetic studies (*16*) may be involved in binding the arginine in P-2 rather than catalysis (*21*). These data indicated either that, if there is a base catalyst in the kinase reaction, its pK_a is lower than 5 or that the burst phase is limited by a metal-dependent conformational change. The weak basicity of the aspartate (pK_a less than 5) compared to the basicity of the serine pK_a 14 led to the suggestion that it may not be an effective general base. Moreover, the tyrosine kinase, Csk, has been shown to have a similar catalytic efficiency with a peptide substrate containing the unnatural amino acid trifluorotyrosine (that exhibits a four-unit change in pK_a of the phenolic

[1] Abbreviations: cAPK, cyclic AMP dependent protein kinase; GP, rabbit muscle glycogen phosphorylase; PhK, residues 1−298 of the catalytic γ subunit of rabbit muscle phosphorylase kinase; PK, pyruvate kinase.

group) as that observed with a natural tyrosine containing substrate, indicating that base catalysis was not obligatory (*18*). To characterize the role of the aspartate in phosphorylase kinase catalysis, we have carried out kinetic studies on mutant forms of the enzyme in which the catalytic aspartate, Asp149, has been replaced with alanine and asparagine. Both mutant enzymes show significant decrease in catalysis in support for a crucial catalytic role of the aspartate residue.

Phosphorylation on a residue (or residues) located in the activation segment at the center of the kinase domain plays a key role in regulation in many signaling protein kinases (*22*). Many of the protein kinases are inactive in the dephospho form but can be activated, often in cascade processes or in auto catalytic events, by phosphorylation on threonine, serine, or tyrosine residues in the activation segment. The activation segment (residues 167−193 in PhK) is defined as the region spanning the conserved sequences DFG (residues 167−169 from subdomain VII) and APE (residues 191−193 from subdomain VIII) [using the single letter amino acid code and the subdomain nomenclature of (*3*)] (Figure 1). Between these conserved motifs, the central part of the activation segment shows considerable sequence variation in the different kinases, and yet the segment plays a crucial role in kinase activation. Structural studies on phospho forms of several kinases have shown that the phospho group is involved in ionic interactions with a cluster of basic residues (*12*, *15*, *23*−*26*). The ionic and hydrogen bond interactions between the phosphate and protein groups serve primarily to localize the activation segment in the region that forms part of the peptide substrate binding site; in addition, they may stabilize interactions between the N-terminal and C-terminal lobes, bringing the ATP binding catalytic residues into their correct positions, and, by promoting a defined conformation of the activation segment, they may relieve steric blocking of the catalytic site. There is no change in position of the catalytic aspartate between the active and inactive forms of these kinases. In each of these structures, one of the important ionic interactions made (either directly or indirectly through water) by the phospho residue involves an arginine that precedes the catalytic aspartate. Titin kinase is an exception to this rule and the first known nonarginine-aspartate kinase to be activated by phosphorylation (*27*).

The critical role for the correct conformation of the activation segment is illustrated by the IRK and PhK peptide complexes where a short stretch of antiparallel β-sheet is formed between the activation segment and the $P + 1$ and $P + 3$ position of the peptide substrate (*10*, *15*). This part of the activation segment has also been implicated in substrate recognition for the proline-$P + 1$ specific kinases CDK2 and MAPK (*24*, *25*). PhK is active without the requirement for phosphorylation of residues in the activation segment. The spatially equivalent residue to that which is phosphorylated in other kinases is a glutamate in PhK, Glu182 (*8*). The activation segment is stabilized by the interaction of the glutamate with the arginine that precedes the catalytic aspartate. The cluster is further linked by hydrogen bonds to a tyrosine, Tyr206 (Figure 1). These interactions mimic those made by phospho residues in other protein kinases. To explore the contributions of the activation segment to substrate recognition and catalysis, we have carried out site-directed mutagenesis studies on the glutamate and surrounding interacting residues. The results show a decrease in catalytic efficiency even though the sites that are modified are 12 Å from the site of catalysis. The mutant Glu182Ser has been crystallized, and the crystal structure shows negligible change in structure from the wild-type enzyme. A phosphate ion is interposed between the mutated serine and the arginine resulting in a similar conformation for the activation segment.

MATERIALS AND METHODS

Site-directed mutagenesis of the PhK cDNA was carried out by megaprimer polymerase chain reactions and the gene subsequently cloned into the vector pMW172 (*28*) using *Nde*I (5′) and *Hin*dIII (3′) restriction sites. The native PhK and the mutant enzymes were expressed in BL21DE3 plysS cells as inclusion bodies followed by renaturation and purification by DEAE ion exchange (Q Sepharose, Pharmacia) and Cibacron blue affinity chromatography (Sigma) as described previously (*7*).

AMP, ATP, glucose 1-phosphate (dipotassium salt), β-glycerophosphate, glycogen, NADH, pyruvate kinase, lactate dehydrogenase, phosphoenolpyruvate, and other chemicals were obtained from Sigma. Oyster glycogen was freed of AMP by the method of Helmreich and Cori (*29*). Glycogen phosphorylase b (GPb) was isolated from rabbit skeletal muscle as previously described (*30*). Its concentration was determined from absorbance measurements at 280 nm using an absorbance index $A^{1\%}_{1cm} = 1.32$ (*31*). PhK concentration was determined according to Bradford (*32*). The MC-peptide Ac−RQMSFRL was synthesized on an Applied Biosystems 430A Automated Peptide Synthesizer, using Fmoc methodology.

Relative Viscosity Measurements. The relative viscosity (η_{rel}) of the reaction mixtures containing sucrose as a viscosogen was measured relative to the reaction buffer (50 mM Tris, 50 mM Hepes, 0.5 mM calcium chloride, 2 mM DTT, and 10 mM magnesium acetate, pH 8.2), at 30 °C, using a Cannon-Fenske Routine viscometer. Sucrose concentrations 10, 20, 25, and 30% resulted in relative viscosities of 1.23, 1.67, 1.91, and 2.31, respectively. All measurements were performed in triplicate.

Enzyme Assays. The enzymic activity of PhK and its mutants was measured by monitoring the conversion of GPb to GPa by assaying phosphorylase activity in the presence of 10 μM AMP and 0.5 mM caffeine (*33*, *34*) in the direction of glycogen synthesis. All reactions were performed at 30 °C. The total volume of the enzymic reaction mixtures was 0.2 mL and contained buffer (50 mM Tris, 50 mM Hepes, 0.5 mM calcium chloride, 2 mM DTT, 10 mM magnesium acetate, and 0.5 mg/mL BSA, pH 8.2), various GPb concentrations (0.5−10 mg/mL), and saturating concentration of ATP (1.5 mM for the native, Asp149Asn and Glu182Ser, 3 mM for Tyr206Phe and Arg148Ala, and 5 mM for the Asp149Ala mutants) or various ATP concentrations (0.06−3 mM) in saturating concentration of GPb (5−10 mg/mL). The mixtures were incubated for 1 min at 30 °C, and the reaction was initiated by the addition of 5−10 ng/mL PhK (55 μg/mL for Asp149Ala and 25 μg/mL for Asp148Asn). At times 4, 8, 12, and 14 min, samples were withdrawn, and the reaction was stopped by 50 times dilution in buffer containing 100 mM triethanolamine/HCl (pH 6.8), 1 mM EDTA, and

2 mM DTT at 0 °C. In the phosphorylase assay, initial reaction rates were measured at pH 6.8 and 30 °C by the release of orthophosphate from glucose-1-P. The GPa was assayed in 50 mM triethanolamine/HCl, 0.5 mM EDTA, 1 mM DTT, 1% glycogen, 76 mM Glc-1-P, 10 μM AMP, and 0.5 mM caffeine. Samples were withdrawn after 14 min and transferred into 0.2% sodium dodecyl sulfate to stop the reaction. Inorganic phosphate released in the phosphorylase reaction was determined, and initial rates were calculated as described (*35*). Kinetic data were analyzed by the use of the nonlinear regression program GRAFIT (*36*).

The enzymic activity of PhK in several relative viscosity buffers was measured by monitoring the conversion of GPb to GPa as previously described. The assay was performed, in the presence and the absence of sucrose as the viscosogen, with respect to GPb concentrations (1−10 mg/mL) and saturating concentration of ATP (1.5 mM) and various ATP concentrations (0.06−1.5 mM) in nonsaturating and saturating concentrations of GPb 0.5 and 5 mg/mL, respectively. Some variation in kinetic parameters k_{cat} and K_m was observed for different enzyme preparations. However, within each preparation, the means of the standard errors for the calculated k_{cat} and K_m values averaged less than 10% for a period of 2 months.

The phosphorylation of the MC-peptide by the PhK in several relative viscosity buffers was measured spectrophotometrically according to an assay (*37*, *38*) in which ADP production is coupled through the reaction of the kinase to the NADH oxidation by pyruvate kinase (PK) and lactate dehydrogenase (LDH), with minor modifications. The NADH consumption during the reaction results in a decrease in absorbance at 340 nm. All enzymic reactions were performed at 30 °C. The assay mixture contained, in a 0.3 mL total volume, buffer (50 mM Tris, 50 mM Hepes, 0.5 mM calcium chloride, 2 mM DTT, and 10 mM magnesium acetate, pH 8.2), in the presence or absence of sucrose, 0.1 mg/mL BSA, 3.6 units of LDH, 1.2 units of PK, 1 mM phosphoenolpyruvate, and 0.2 mM NADH. The concentration of the MC-peptide varied from 0.1 to 1.5 mM. The reaction was initiated by the simultaneous addition of the PhK and ATP (final concentration in the reaction mixture 0.5 μg/mL and 1 mM, respectively). Samples were withdrawn at 0.5 min intervals over the period from 5 to 15 min and transferred into 0.1% sodium dodecyl sulfate (final concentration) to terminate the reaction. Absorbance was measured at 340 nm. A molar extinction coefficient of 6220 M^{-1} cm^{-1} for NADH at 340 nm was used in the calculations. The PhK activity with respect to ATP varying from 0.04 to 1 mM and 0.4 mM of MC-peptide was also assayed in the presence or absence of sucrose. A control sample was used for each ATP concentration containing the reaction mixture without PhK, to record any background ATP hydrolysis, mainly due to the ATPase activity of PK. The reaction rates were independent of the PK and LDH concentrations and varied linearly with the concentration of the PhK.

ATPase activity was measured by using the enzyme-coupled assay (described above). All enzymic reactions were performed at 30 °C. The assay mixture (1.0 mL) contained PhK or Asp149Ala or Asp149Asn mutant PhKs (30 μg/mL), 1.5 mM ATP, the reaction's buffer (50 mM Tris, 50 mM Hepes, 0.5 mM $CaCl_2$, 2 mM DTT, and 10 mM magnesium acetate, pH 8.2), 0.2 mg/mL BSA, 30 units of LDH, 10 units of PK, 1 mM phosphoenolpyruvate, and 0.3 mM NADH. The reaction was started by adding kinase/ATP mixture. Samples (0.3 mL) were withdrawn at 4, 10, and 30 min and transferred to 0.3 mL sodium dodecyl sulfate 0.2% (w/v) to stop the reaction. Absorbance was measured at 340 nm.

Glu182Ser Crystallography. Crystals of Glu182Ser PhK were grown under conditions similar to those published for the wild-type PhK (*8*), in the presence of AMPPNP (3 mM) and $MnCl_2$ (10 mM). Only small crystals could be grown, necessitating data collection at a synchrotron radiation source for which there was some delay before time was available. Data were collected to 2.3 Å resolution on beam line ID3 at the ESRF, Grenoble. The structure of Glu182Ser PhK was refined using the programs O (*39*) and REFMAC (*40*), starting from the coordinates of PhK in ternary complex with peptide and AMPPNP (*10*). This structure, solved at a resolution of 2.6 Å, was chosen as the starting model over the slightly higher resolution (2.1 Å) PhK binary complex structure, which was also available because certain loops are better ordered in the peptide-bound structure. Initially, rigid body refinement was carried out using a single rigid body with subsequent cycles with increasing number of fragments to a limit of fragments of 20 residues. As the number of rigid bodies was increased, so the resolution of the data included was increased from initially 3.5 to finally 2.3 Å. Subsequent refinement was performed using anisotropic scaling with bulk solvent correction and the maximum likelihood target function. Waters were included by adoption from the refined 2.1 Å native PhK structure.

RESULTS

Effects of Viscosity on Steady-State Kinetic Parameters. Detailed analysis of cAPK kinetics has shown that the reaction proceeds with a fast chemical step followed by release of product in which release of ADP is the rate-limiting step (*19*, *41*). Adams and colleagues have used variation in solvent viscosity to probe the diffusion-controlled limits for cAPK catalyzed reaction. We have used a similar strategy to analyze the effects of viscosity on the steady-state kinetic parameters for wild-type PhK-catalyzed phosphorylation of GPb and the MC-peptide. The dependence of k_{cat} and k_{cat}/k_m on viscosity is shown in Figure 2 and summarized in Table 1. In each experiment, a linear dependence of kinetic parameters on relative viscosity η^{rel} was observed. $(k_{cat})^{\eta}$ and $(k_{cat}/K_m)^{\eta}$ are the slopes of the plots k^0_{cat}/k_{cat} vs η^{rel} and $(k_{cat}/K_m)^0/(k_{cat}/K_m)$ vs η^{rel}, where k^0_{cat}/k_{cat} and $(k_{cat}/K_m)^0/(k_{cat}/K_m)$ are the relative values of k_{cat} and k_{cat}/K_m in the absence and presence of the viscosogen, respectively. At saturating ATP (1.5 mM) and with variable GPb, $(k_{cat})^{\eta}$ and $(k_{cat}/K_m)^{\eta}$ were close to 1.0 (1.10 ± 0.17 and 0.93 ± 0.04, respectively). Likewise, at saturating GPb (5 mg/mL; 50 μM) and variable ATP, the slopes of $(k_{cat})^{\eta}$ and $(k_{cat}/K_m)^{\eta}$ were 1.08 ± 0.15 and 1.05 ± 0.13, respectively. At low GPb concentration (0.5 mg/mL; 5 μM) and variable ATP, the slopes were 0.89 ± 0.08 and 0.96 ± 0.10 while for low ATP concentration (0.06 mM), and at variable GPb, the slopes were 1.00 ± 0.06 and 1.02 ± 0.04, respectively. With the MC-peptide substrate, which is a poor substrate, there was no change in the relative values of the kinetic parameters k^0_{cat}/k_{cat} and $(k_{cat}/K_m)^0/(k_{cat}/K_m)$ with viscosity.

The steady-state kinetic analysis suggests a random bi−bi kinetic mechanism similar to that proposed by Tabatabai

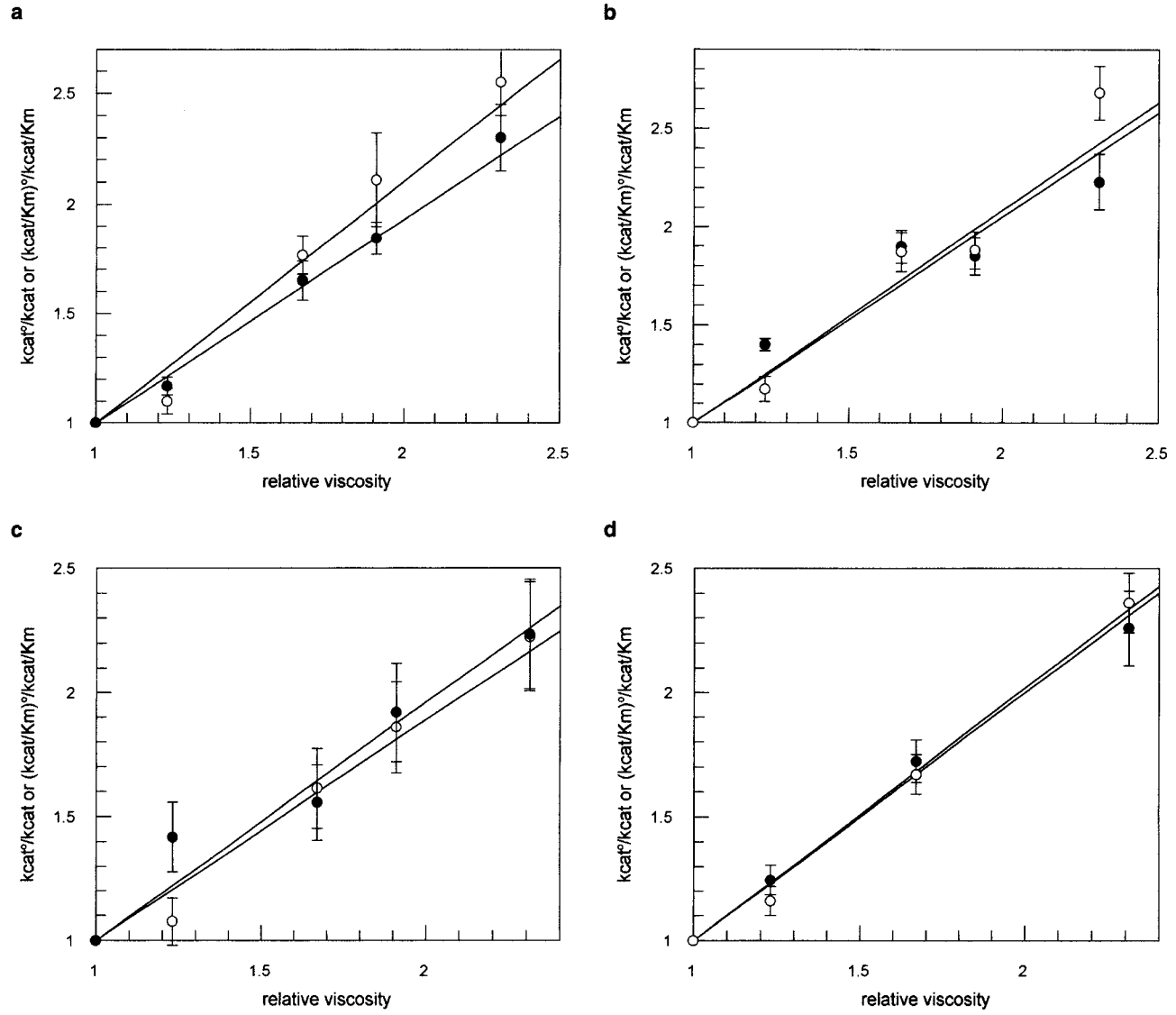

FIGURE 2: Dependence of the steady-state kinetic parameters for GPb on the relative viscosity of the solution (50 mM Tris, 50 mM Hepes, 0.5 mM $CaCl_2$, 2 mM DTT, 10 mM magnesium acetate, pH 8.2, 30 °C). k^0_{cat}/k_{cat} (○) and $(k_{cat}/K_m)^0/(k_{cat}/K_m)$ (●) are the ratios of the observed k_{cat} and k_{cat}/K_m values in the absence and presence of sucrose, respectively. (a) Variable GPb (where [GPb] = 0.5−10 mg/mL) and saturating ATP ([ATP] = 1.5 mM). The slope of the k^0_{cat}/k_{cat} is 1.10 ± 0.17 and that of $(k_{cat}/K_m)^0/(k_{cat}/K_m)$ is 0.93 ± 0.04. (b) Saturating GPb (where [GPb] = 5 mg/mL) and variable ATP ([ATP] = 0.06−1.5 mM). The slope of the k^0_{cat}/k_{cat} is 1.084 ± 0.15 and that of $(k_{cat}/K_m)^0/(k_{cat}/K_m)$ is 1.05 ± 0.13. (c) Low GPb (where [GPb] = 0.5 mg/mL) and variable ATP ([ATP] = 0.06−1.5 mM). The slope of k^0_{cat}/k_{cat} is 0.89 ± 0.080 and that of $(k_{cat}/K_m)^0/(k_{cat}/K_m)$ is 0.96 ± 0.10. (d) Low ATP (where [ATP] = 0.06 mM) and variable GPb ([GPb] = 0.5 mg/mL = 10 mg/mL). The slope of the k^0_{cat}/k_{cat} is 1.00 ± 0.06 and that of $(k_{cat}/K_m)^0/(k_{cat}/K_m)$ is 1.02 ± 0.04.

Table 1: Steady-State Kinetic Parameters and Viscosity Effects for Phosphorylase Kinase Substrates[a]

substrate (varied ligand)	k_{cat} (s^{-1})	K_m (μM)	k_{cat}/K_m ($\mu M^{-1} s^{-1}$)	$(k_{cat})^\eta$	$(k_{cat}/K_m)^\eta$
GP*b* (GPb)[b]	28.6 ± 2.3	5.3 ± 0.1	5.39 ± 0.43	1.10 ± 0.17	0.93 ± 0.04
GP*b* (ATP)[c]	28.0 ± 2.0	70.9 ± 6.5	0.39 ± 0.03	1.08 ± 0.15	1.05 ± 0.13
GP*b* (ATP)[d]	12.3 ± 0.2	65.0 ± 6.0	0.19 ± 0.02	0.89 ± 0.08	0.96 ± 0.10
GP*b* (GPb)[e]	13.3 ± 0.4	4.9 ± 0.8	2.70 ± 0.20	1.00 ± 0.06	1.02 ± 0.04
MC-peptide (MC-peptide)[f]	7.5 ± 0.16	257.5 ± 121	0.029	0	0
MC-peptide (ATP)[g]	8.0 ± 0.36	87.3 ± 14.3	0.092	0	0

[a] $(k_{cat})^\eta$ and $(k_{cat}/K_m)^\eta$ are the slopes of the plots of the k^o_{cat}/k_{cat} and $(k_{cat}/K_m)^o/(k_{cat}/K_m)$ versus the relative viscosity. The steady-state kinetic data were determined from plots of initial velocity versus substrate concentration according to Michaelis−Menten equation. The assay conditions are described in the Materials and Methods. [b] [GPb] varied (0.5−10 mg/mL) and [ATP] was 1.5 mM. [c] [ATP] varied (0.06−1.5 mM) and [GPb] was 5 mg/mL. [d] [ATP] varied (0.06−1.5 mM) and [GPb] was 0.5 mg/mL. [e] [GPb] varied (0.5−10 mg/mL) and [ATP] was 0.06 mM. [f] [MC-peptide] varied (0.1−1.5 mM) and [ATP] was 1 mM. [g] [ATP] varied (0.04−0.1 mM) and [MC-peptide] was 0.4 mM.

and Graves (*42*), which is shown in Table 2. ATP at saturating concentrations combines with the enzyme to form the E·ATP complex with second-order association rate constant k_1 and dissociation rate constant k_{-1}. Studies on protein kinases have indicated that although the reaction proceeds in random sequential mechanism, there is a

Table 2: Estimates of the Microscopic Rate Constants for the Kinetic Scheme from Viscosity Measurements

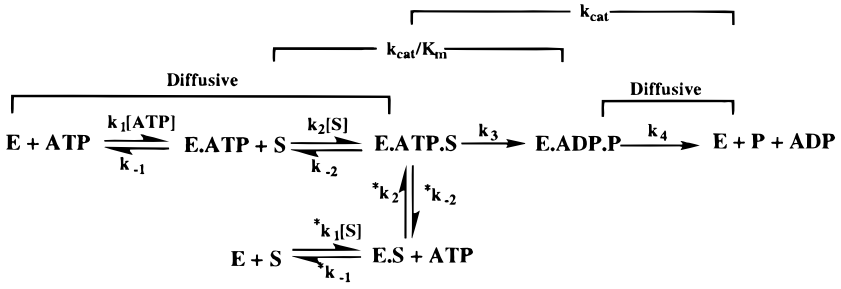

$k_1 = 0.2 \pm 0.03\ \mu M^{-1}\ s^{-1}$ calcd from eqs 5 and 6 for nonsaturating conditions
$k_2 = 5.79 \pm 0.5\ \mu M^{-1}\ s^{-1}$ calcd from eqs 2 and 4 when [ATP] is saturating
$k_3 \geq 360\ s^{-1}$ estimated from eq 1 using error limits on slopes
$k_4 = 28.6 \pm 2.3\ s^{-1}$
$k_{-1} \leq 16.8\ s^{-1}$ calcd from eq 6 for nonsaturating [GPb]
$k_{-2} \geq 27\ s^{-1}$ from eq 4 when [ATP] is saturating
$k_{-1} / k_1 \leq 84\ \mu M$
$k_{-2}/k_2 \geq 4.7\ \mu M$
$^*k_1 = 2.7 \pm 0.2\ \mu M^{-1}\ s^{-1}$ from eqs 5 and 6 when [ATP] is low
$^*k_2 = 0.39 \pm 0.03\ \mu M^{-1} s^{-1}$ from eqs 2 and 4 when GPb is saturated
$^*k_{-1} = 15.8\ s^{-1}$ from eqs 5 and 6 when [ATP] is low
$^*k_{-2} \leq 32.8\ s^{-1}$ as estimated from eq 4 when GPb is saturated
$^*k_{-1} / ^*k_1 = 5.8\ \mu M$
$^*k_{-2} / ^*k_2 \leq 84\ \mu M$

preference for ATP binding first at high ATP concentrations (*20*). The protein or peptide substrate (S) combines with the E·ATP complex to form the ternary enzyme−substrate complex E·ATP·S with association and dissociation rate constants k_2 and k_{-2}. When the substrate is at saturating concentrations (especially for GPb since it has a higher affinity for the enzyme than ATP), the enzyme may combine first with the protein or peptide substrate to form the E·S complex with association rate constant $^*k_1$ and dissociation rate constant $^*k_{-1}$. ATP in turn, combines with the E·S complex, and the E·ATP·S complex is formed with association and dissociation rate constants $^*k_2$ and $^*k_{-2}$, respectively. Once the ternary complex E·ATP·S is formed, the chemical phosphoryl transfer step (assumed to be irreversible) follows, in which the γ-phosphate of ATP is transferred to the serine hydroxyl group with a unimolecular rate constant k_3. The enzyme-ADP-phosphoryl-substrate complex then dissociates. In cAPK, the phosphoryl-peptide (*P*) dissociation is assumed to occur first (*20*, *37*). The rate-limiting step in the reaction pathway is then the dissociation of the E·ADP complex. A similar analysis is not available for PhK, and we assume k_4 includes the overall rate of product release and possibly viscosity dependent conformational changes.

The steady-state parameters are related to the microscopic rate constants by

$$k_{cat} = k_3 k_4/(k_3 + k_4) \quad (1)$$

$$k_{cat}/K_m = k_2 k_3/(k_{-2} + k_3) \quad (2)$$

The rate constants k_{-1}, k_{-1}, $^*k_1$, $^*k_{-1}$, k_2, k_{-2}, $^*k_2$, and $^*k_{-2}$ as well as k_4 represent diffusion controlled processes and these rate constants will be sensitive to the viscosity of the solvent, while k_3, the unimolecular step, is assumed to be independent of viscosity. Using these equations and following Adams and Taylor (*19*) assuming the diffusion controlled rate constants are inversely related to the viscosity of the solution, the slopes of the plots of k^0_{cat}/k_{cat} and $(k_{cat}/K_m)^0/(k_{cat}/K_m)$ versus relative viscosity, η^{rel} are given by

$$(k_{cat})^\eta = k_3/(k_3 + k^0_4) \quad (3)$$

$$(k_{cat}/K_m)^\eta = k_3/(k^0_{-2} + k_3) \quad (4)$$

where k^0_{-2} and k^0_4 are the dissociation rate constants for substrate and products, respectively, when $\eta^{rel} = 1$. When the chemical step is much faster than the release of products (i.e., $k_3 \gg k_4$), $(k_{cat})^\eta$ approaches the limiting value of 1 and $k_{cat} = k_4$. If the dissociation of products is fast compared to the chemical step (i.e., $k_4 \gg k_3$) then there are no viscosity effects and $(k_{cat})^\eta = 0$. Likewise, when the substrate binds tightly to the enzyme (i.e., $k_3 \gg k^0_{-2}$), $(k_{cat}/K_m)^\eta$ approaches the limit of 1 and $k_{cat}/K_m = k_2$.

A summary of the kinetic constants calculated for PhK is given in Table 2. For saturating ATP (1.5 mM) and variable GPb, the value of $(k_{cat})^\eta$ is close to 1, indicating that the chemical step is much faster than the dissociation of products and that the latter step is represented by $k_{cat} = k_4 = 28.6\ s^{-1}$. Only a lower limit can be assigned to k_3 (i.e., $k_3 \geq 360\ s^{-1}$) as estimated from the eq 1 given the error limits of the slopes of the viscosity plots. Likewise, $(k_{cat}/K_m)^\eta$ is also close to 1, hence $(k_3 \gg k_{-2})$, indicating that GPb is a "sticky" substrate and that the second-order association rate constant $k_2 = k_{cat}/K_m = 5.79 \pm 0.5\ \mu M^{-1}\ s^{-1}$. At saturating GPb (5 mg/mL) and variable ATP, the value of $(k_{cat})^\eta$ is close to 1, and hence $k_{cat} = k_4 = 28\ s^{-1}$, in agreement with the value found for saturating ATP and variable GPb concentrations. The value of $(k_{cat}/K_m)^\eta = 1.05$, and hence $^*k_2 = 0.39\ \mu M^{-1}\ s^{-1}$. In addition $^*k_{-2} \ll k_3$, suggesting a nonrapid equilibrium binding of ATP. The k_{-2}/k_2 ($\geq 4.7\ \mu M$) and $^*k_{-2}/^*k_2$ ($\leq 84\ \mu M$) values as calculated from the kinetic estimates (Table 2) are consistent with K_m when ATP and GPb are at saturating concentrations [5.3 μM and 70.9 μM, respectively (Table 1)].

For nonsaturating conditions, the steady-state parameters are related to the microscopic rate constants by the

Table 3: Kinetic Parameters of PhK and Mutant Enzymes

	[GPb] variable substrate			[ATP] variable substrate		
enzyme	k_{cat} (s^{-1})	K_m (μM)	k_{cat}/K_m ($\mu M^{-1} s^{-1}$)	k_{cat} (s^{-1})	K_m (μM)	k_{cat}/K_m ($\mu M^{-1} s^{-1}$)
WT	66.7 ± 2	8.9 ± 0.6	7.5	56.7 ± 2	105 ± 10	0.54
D149A	.005	34.9 ± 4.6	1.4×10^{-4}	.0043	930 ± 31	4.6×10^{-6}
D149N	0.013 ± 0.001	10.3 ± 0.5	1.26×10^{-3}	0.013 ± 0.001	123 ± 12.6	1.1×10^{-4}
E182S	3.3 ± 0.3	17.8 ± 0.3	0.18	3.0 ± 0.3	135 ± 14	0.02
R148A	15 ± 2	18.6 ± 3.4	0.80	10.0 ± 2	316 ± 10	0.03
Y206F	6.7 ± 0.2	12.6 ± 1.2	0.53	6.2 ± 0.2	221.0 ± 13	0.03

following equations:

$$k_{cat}/K_m = [(k_1k_3[S])/(k_{-2}/k_2)]/[k_3[S]/(k_{-2}/k_2) + k_{-1}] \quad (5)$$

while the sensitivity of the $(k_{cat}/K_m)^\eta$ to the viscosity is expressed by

$$(k_{cat}/K_m)^\eta = [(k_3[S])/(k_{-2}/k_2)]/[k_3[S]/(k_{-2}/k_2) + k_{-1}] \quad (6)$$

The association and dissociation rate constants k_1 and k_{-1} of the E·ATP transient complex as well as the rate constants $*k_1$ and $*k_{-1}$ of the E·S complex can be estimated by solving the above eqs 5 and 6 for nonsaturating GPb and ATP concentrations, respectively. For low GPb concentration 0.5 mg/mL and variable ATP, $(k_{cat}/K_m)^\eta$ is close to 1, hence the second-order association constant $k_1 = k_{cat}/K_m = 0.2\ \mu M^{-1}\ s^{-1}$. k_{-1} has an upper limit of 16.8 s^{-1}. Similarly, $(k_{cat}/K_m)^\eta$ is 1 when ATP concentration is low (0.06 mM) and variable GPb, thus the equivalent association constant $*k_1 = k_{cat}/K_m = 2.7\ \mu M^{-1}\ s^{-1}$, and the $*k_{-1}$ estimated 15.8 s^{-1}.

For the MC-peptide, both $(k_{cat})^\eta$ and $(k_{cat}/K_m)^\eta$ are zero, indicating that there are no viscosity effects. The lack of a viscosity effect with this substrate formed an important control, for it showed that the viscosogens are not general inhibitors of the enzyme reaction. With the poor MC-peptide substrate, the rate constant for the dissociation is greater than the rate constant for the chemical step ($k_4^0 > k_3$). Solving the eqs 1 and 2, assuming that the rate constant for dissociation of products is the same as in the case of the saturating ATP example (i.e., $k_4 = 28.6\ s^{-1}$),then k_3=7.5 s^{-1}. There is also rapid equilibrium binding of the substrate so that $k_{-2}^0 \gg k_3$.

Steady-State Kinetics Parameters for Asp149 Mutant PhKs. The kinetic parameters for the Asp149Asn and Asp149Ala mutant PhKs are summarized in Table 3 and compared with those for wild-type PhK. There was some variation in kinetic parameters for wild-type PhK compared with Table 1 due to a different enzyme preparation, as discussed in the Methods section.

The mutant Asp149Ala showed negligible activity with a reduction in k_{cat} by 1.3 10^4, a 4-fold increase in K_m for GPb and a 9-fold increase in K_m for ATP. The Asp149Ala mutant expressed well in *Escherichia coli* cells, and in general, it was found that the less active the mutant PhK, the better the expression. Active PhK appears toxic to cells (*7*). As discussed below, Asp149 is involved in a hydrogen-bonding network. To investigate whether removal of the charge but retention of the hydrogen-bonding network affected kinetic parameters, the mutant Asp149Asn was prepared. This mutant showed a reduction in k_{cat} by 4.5×10^3 and only small changes in K_m (0.7- and 1.1-fold for GPb and ATP, respectively).

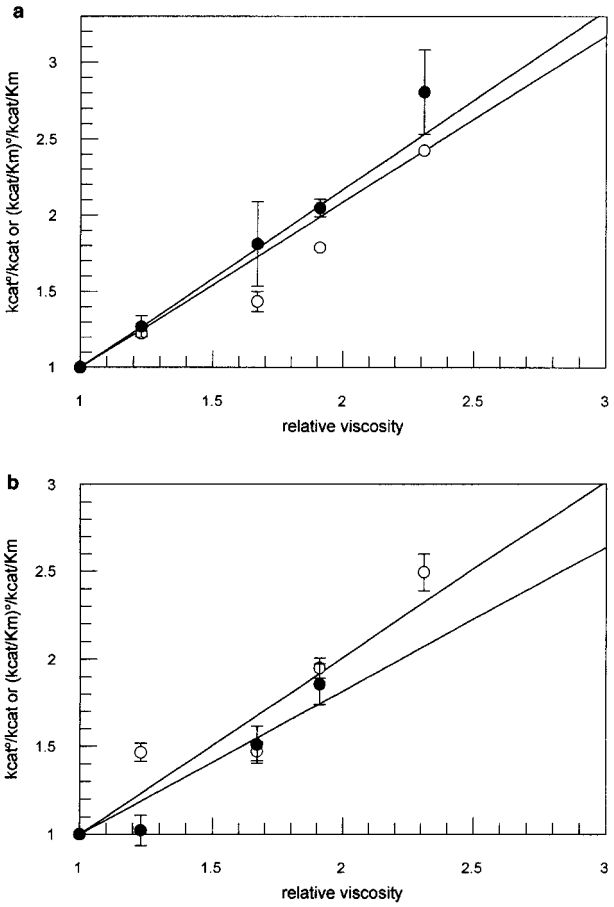

FIGURE 3: Dependence of the steady-state kinetic parameters of the Asp149Asn mutant PhK for GPb on the relative viscosity of the solution (50 mM Tris, 50 mM Hepes, 0.5 mM $CaCl_2$, 2 mM DTT, 10 mM magnesium acetate, pH=8.2, 30 °C). k_{cat}^0/k_{cat} (○) and $(k_{cat}/K_m)^0/(k_{cat}/K_m)$ (●) are the ratios of the observed k_{cat} and k_{cat}/K_m values in the absence and presence of sucrose, respectively. (a) Variable GPb (where [GPb] = 0.5−5 mg/mL), and saturating [ATP] = 1.5 mM). The slope of the k_{cat}^0/k_{cat} is 1.09 ± 0.01 and that of $(k_{cat}/K_m)^0/(k_{cat}/K_m)$ is 1.15 ± 0.01. (b) Saturating GPb (where [GPb] = 5 mg/mL) and variable [ATP] (where [ATP] = 0.06−1.5 mM). The slope of the k_{cat}^0/k_{cat} is 1.01 ± 0.15 and that of $(k_{cat}/K_m)^0/(k_{cat}/K_m)$ is 0.82 ± 0.15.

To assess if there had been a change in the kinetic mechanism with the Asp149Asn mutant, we examined the kinetic parameters as a function of viscosity as shown in Figure 3. The analysis of these data (summarized in Table 4) is less precise than for the native PhK, because the activity is low. From Figure 3a with variable GPb concentrations, the value of $(k_{cat})^\eta = 1.09 \pm 0.01$, indicating that the chemical step is still faster than the dissociation of products and that the latter is represented by $k_{cat} = k_4 = 0.013\ s^{-1}$. Using the error limits for $(k_{cat})^\eta$, we estimate that $k_3 \geq 0.08\ s^{-1}$. From

Table 4: Comparison of Kinetic Parameters for Wild-Type and Asp149 Mutant PhKs

	wild-type	Asp149Asn
k_2 (μM^{-1} s^{-1})	5.79 ± 0.5	$1.26 \times 10^{-3} \pm 6.4 \times 10^{-5}$
k_3 (s^{-1})	≥ 360	≥ 0.08
k_4 (s^{-1})	28.6 ± 2.3	0.013
$*k_2$ (μM^{-1} s^{-1})	0.39 ± 0.03	$1.28 \times 10^{-4} \pm 2.7 \times 10^{-5}$
$*k_{-2}$ (s^{-1})	≤ 32.8	≥ 0.02
$*k_{-2}/*k_2$ (μM)	≤ 84	≥ 160

ATPase activity	k_{cat} (s^{-1})
wild-type	0.23
Asp149Asn	0.052
Asp149Ala	0.005

Figure 3a, $(k_{cat}/K_m)^{\eta} = 1.15 \pm 0.01$, suggesting that $k_3 \gg k_{-2}$ and the second-order association constant for GPb $k_2 = k_{cat}/K_m = 1.26 \times 10^{-3} \pm 6.4\ 10^{-5}\ \mu M^{-1}\ s^{-1}$. Since the value of $(k_{cat}/K_m)^{\eta}$ is greater than 1, k_{-2} cannot be calculated. For variable ATP and saturating GPb (Figure 3b), again $(k_{cat})^{\eta}$ is close to 1, giving $k_4 = 0.013\ s^{-1}$. $(k_{cat}/K_m)^{\eta} = 0.82 \pm 0.15$, and solving eqs 4 and 2, the second-order dissociation rate constant for ATP $*k_2 = 1.28 \times 10^{-4} \pm 2.7 \times 10^{-5}\ \mu M^{-1}\ s^{-1}$. These values for k_2 and $*k_2$ are very much smaller than the corresponding values for the wild-type PhK. Using the estimate $k_3 \geq 0.08\ s^{-1}$, $*k_{-2} \geq 0.02\ s^{-1}$ and $*k_{-2}/*k_2 \geq 160\ \mu M$, indicating slightly weaker binding of ATP to the Asp149Asn mutant than the native PhK.

We measured the ATPase activities of the aspartic acid mutants in order to compare the relative efficiencies of the mutants to promote the attack of water on ATP (Table 4). The ATPase activity of the wild-type PhK has a $k_{cat} = 0.23\ s^{-1}$, approximately 0.4% of the kinase activity with phosphorylase. The ATPase activity of the Asp149Asn mutant is $0.052\ s^{-1}$, a 4.4-fold reduction compared to wild-type ATPase activity, and for the Asp149Ala mutant, it is $0.005\ s^{-1}$, corresponding to a 46-fold reduction compared to wild-type ATPase activity. The reductions observed in ATPase activities of the Asp149 mutants, where the transfer is to water, are much less than the reduction in kinase activities.

Steady-State Kinetic Parameters for Activation Segment Mutant PhKs. Figure 4 presents a view of some of the interactions of the activation segment with key residues at the catalytic site of PhK. In the activation segment, the glutamate that mimics the phospho residue in other protein kinases, Glu182, interacts with Arg148, the arginine that precedes the catalytic aspartate, Asp149. The distance from Glu182 OE1 to Asp149 OD2 is 12 Å. Arg148 also interacts with Tyr206, a residue that is present in many but not all protein kinases.

Three mutants were prepared to assess the contributions of the glutamate (Glu182) to the stabilization of the activation segment. Kinetic parameters are summarized in Table 3. The Glu182Ser mutant results in a decrease in catalytic efficiency. There is an approximate 20-fold decrease in $k_{cat,}$ a 1.3-fold increase in K_m for ATP, a 2-fold increase in K_m for GPb and a 40-fold decrease in k_{cat}/K_m for GPb. Disruption of the arginine part of the Arg148/Glu182 ion pair in the Arg148Ala mutant resulted in changes in kinetic parameters that showed a similar trend to those observed for the Glu182Ser mutant. There is an approximate 5-fold decrease in k_{cat}, a 3-fold increase in K_m for ATP, a 2-fold increase in K_m for GPb, and an 18-fold decrease in k_{cat}/K_m. Tyr206 also plays a role in the charge−charge interaction through its interaction with Arg148. The small change of tyrosine to phenylalanine, that removes the hydrogen bond to the arginine, had almost as profound effects on the catalytic parameters as those observed for either the glutamate or arginine mutations. The Tyr206Phe mutant has a 9-fold reduction in k_{cat}, a 2-fold increase in K_m for ATP, a 1.4-fold increase in K_m for GPb, and a 14−18-fold decrease in k_{cat}/K_m, indicating that the disruption of the tyrosine hydrogen bond is as deleterious as the other interactions that play a role in stabilizing the activation segment.

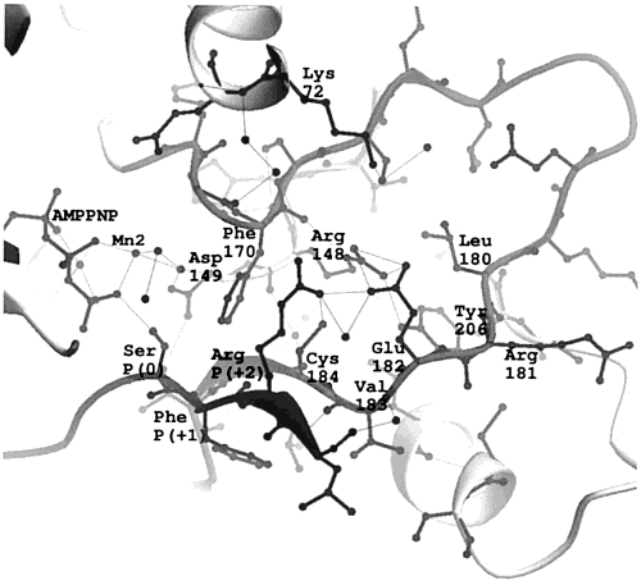

FIGURE 4: Details of the contacts made by Glu182 from the activation segment. The peptide substrate is shown in black with residues numbered P(0), P(+1), and P(+2). The diagram is depth cued so that atoms further from the viewer are in lighter color. Diagram by OGLOBJECTS (M.E.M.N., unpublished material).

Table 5: Data Collection and Refinement Statistics for the Glu182Ser Mutant PhK

data collection	
resolution 20−2.4 Å (highest resolution shell 2.53−2.4 Å)	
no. of observations	40 795
no. of reflections	12 745
completeness	86.6% (78.5%)
mean I/mean $\sigma(I)$	10.1 (2.9)
R_{sym}	4.8% (22.1%)
refinement	
no. of atoms (mean B)	
protein	2279 (55.8 Å^2)
ATP/Mn/phosphate	38 (44.2 Å^2)
waters	104 (57.2 Å^2)
R-factor	25.1%
R_{free}	33.2%
RMS deviation from ideal bond lengths	0.013 Å
RMS deviation from ideal angles	2.7°

Crystal Structure of Glu182Ser Mutant PhK. To check if mutations in residues of the activation segment resulted in significant changes in structure, the mutant Glu182Ser PhK was crystallized, and the crystal structure determined. Data collection and refinement statistics are summarized in Table 5. The limited completeness of the available data prevented a thorough refinement. Only 83 waters were included, and cycles of REFMAC were halted after the R-factor reached 24%. At this stage, the free R-factor was 33%, and ceased to decrease. These high values reflect a large amount of

flexibility observed in the protein, as seen for the peptide-free wild-type PhK structure (*8*). Overall, the structure of the mutant was identical to that of the native PhK. Both proteins are in binary complex with AMPPNP and Mn^{2+}. The rms deviation in Cα coordinates for the whole molecule (274 atoms) was 0.41 Å, with the greatest differences occurring in flexible exposed loops such as the region of residues 52−65 (between β3 and αC).

Immediately after rigid body refinement, SigmaA (*43*) weighted $F_o - F_c$ maps identified a large electron density feature disjoint from the protein in the neighborhood of the mutation. This density was about 2.8 Å from the position that would be occupied by the carboxyl group of Glu182 from the wild-type protein. It abided up to a contour level of 8 times the RMS deviation of the map (Figure 5a). At this contour level, no other feature can be seen in the map. The extra density was interpreted as a phosphate or sulfate molecule in subsequent refinement. There was also subsidiary density that was modeled with water molecules. No additional phosphate was added during crystallization and nor is any sulfate-dependent step used in purification or crystallization. The most likely possibility is that the enzyme has scavenged either phosphate or α-glycerophosphate from the 50 mM β-glycerophosphate buffer, 10% glycerol solution used in considerable molar excess during the refolding step of PhK from solubilized inclusion bodies (*7*). Measurements showed that the buffer contains about 0.1% free phosphate and about 1% α-glycerophosphate. The dianion is held by interactions with Arg148, Lys72, and contacts to two water molecules, one of which links to the main chain NH groups of Ser182 and Arg181. The contact to Ser182 OG is just too long (3.5 Å) for a hydrogen bond. The positions of Asp149 and the AMPPNP are identical in the native and mutant structures.

In addition to the flexible regions identified in the wild-type structure, the Glu182Ser PhK structure showed small breaks in the electron density of residues toward the end of the activation segment (Figure 5b). Notably, residue 186 is flanked by broken electron density in Glu182Ser PhK, whereas this residue is well defined in wild-type protein. These discontinuities in the electron density are consistent with a relative increase in the disorder of the activation segment C-terminal from the site of mutation, although it cannot be ruled out that they may also be an artifact of the incompleteness of the data.

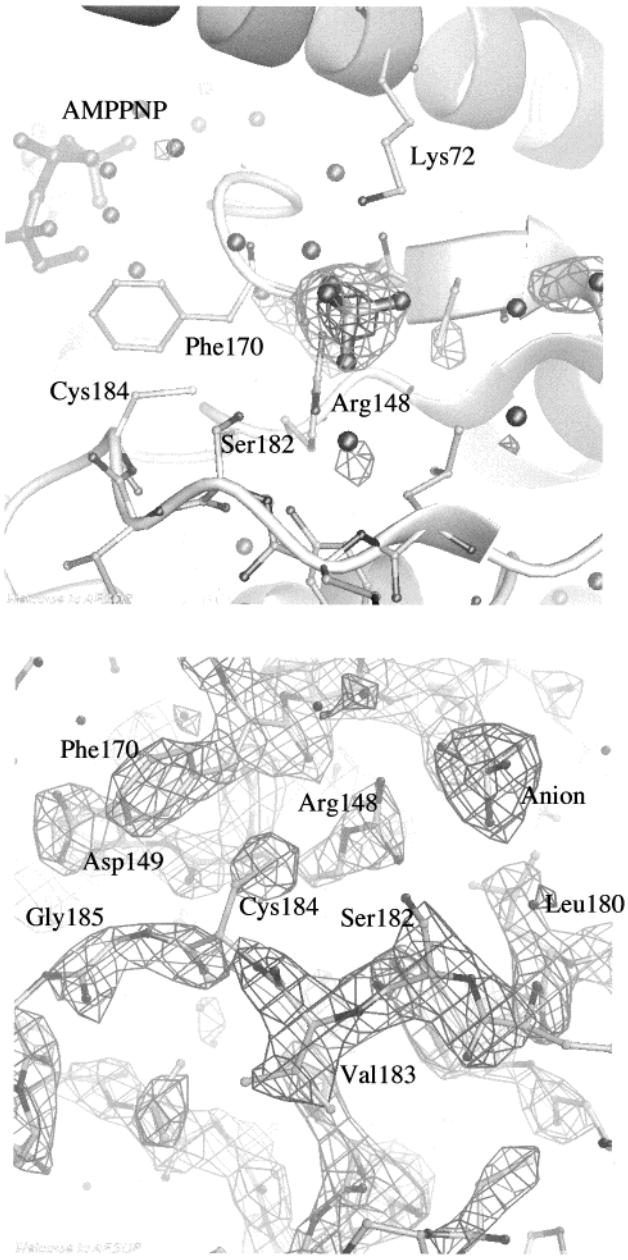

FIGURE 5: Structural results for the Glu182Ser PhK structure. (a) Difference electron density ($F_o - F_c$) contoured at 3σ and 8σ after refinement of the protein structure showing evidence for binding of dianion. (b) Final $2F_o - F_c$ electron density map contoured at 1σ showing poor electron density in the region of Cys184, Gly185, and Thr186, C-terminal to the site of mutation at Glu182Ser. Diagram by OGLOBJECTS (M.E.M.N., unpublished material).

DISCUSSION

The kinetic scheme shown in Table 2 is the minimal mechanistic pathway for the protein kinase reaction. It is, however, almost certainly an oversimplification. Nevertheless, the analysis of the viscosity dependence of the kinetic parameters supports the notion that PhK, like cAPK, follows a reaction in which the chemical step is fast and the rate-limiting step is the dissociation of products from the E·ADP·P complex and/or a viscosity-dependent conformational change. In cAPK, the tighter binding of ADP compared with phosphopeptide suggested that the release of ADP is the rate-limiting step (*41*). There is no direct evidence that this is the case for PhK. Although cAPK and PhK catalytic cores have 33% identity in amino acid sequence and exhibit identical modes of nucleotide and metal binding, suggesting that their mechanisms may also be similar, in cAPK, the nucleotide-binding site is more buried both by the additional C-terminal residues of cAPK and the more closed conformation of the glycine rich loop. In cAPK, prior dissociation of the weakly bound phosphopeptide may well occur before ADP can be released. In PhK, the nucleotide site is more open and we note that the K_i for ADP inhibition of PhK is higher (50 μM) (*44*) than the corresponding inhibition constant for cAPK (7 μM) (*20*). We also note that, although the inhibition constant of GPa for PhK has not been measured, once phosphorylated, the conformation of the N-terminal residues of GPa is not compatible with the catalytic site of PhK (*10*), indicating that conformational strain could provide an incentive for rapid dissociation of the phosphoprotein. For these reasons we can only infer that

k_4 represents the dissociation rate constant for overall release of products. The estimate of product release ($k_4 = k_{cat} = 28$ s^{-1}) is similar to the value reported for cAPK measured under similar conditions (20 s^{-1}) (*19*).

With PhK, we are able only to place a lower limit on the rate of the chemical step represented by k_3 ($k_3 \geq 360$ s^{-1}, as determined from the estimate of errors in the slopes of the viscosity plots). The more detailed analysis of the burst phase kinetics in cAPK gave $k_3 = 500$ s^{-1} for this kinase (*41*). Under conditions of saturating substrates, the estimates of the dissociation constants [K_d (GPb) $= k_{-2}/k_2 \geq 4.7$ μM and K_d (ATP) $= k_{-2}/k_2 \leq 84$ μM] are comparable with K_m values estimated [i.e., K_m(GPb) $= 5.3$ μM and K_m(ATP) $= 70.9$ μM). Likewise the dissociation constants estimated for the binary complexes (PhK·GPb, $*k_{-1}/*k_1 = 5.8$ μM; PhK·ATP, $k_{-1}/k_1 \leq 84$ μM) are similar to the dissociation constants for formation of the respective ternary complexes, indicating, within the limits of error of the analysis, the binding of one substrate does not cause large changes in the binding of the other substrate. The MC-peptide substrate is a poor substrate with K_m value for the peptide 257 μM compared with K_m for GPb of 5.3 μM. There was no change in the relative kinetic parameters as a function of viscosity (Table 1). This could indicate a mechanism in which k_4 is now greater than k_3 and that the chemical step is now significantly impaired. A similar reduced effect of viscosity on the relative kinetic parameters was observed with cAPK with a poor substrate (*21*). The results highlight, as expected, that substrate binding and catalysis are inextricably linked.

Role of the Catalytic Aspartate. The analysis of the Asp149Ala PhK mutant showed that this mutant exhibited negligible activity. There was a major reduction in k_{cat} (1.3×10^4) and 4-fold and 9-fold increase in values for K_m for GPb and ATP, respectively. These changes are more dramatic than those reported by Gibbs et al. (*45*) for yeast cAPK where the mutant Asp210Ala (corresponding to Asp166 in mammalian cAPK) had a 300-fold reduction in k_{cat} and 3- and 1.5-fold increase in K_m for peptide substrate and ATP, respectively. Our results show the critical importance of the aspartate for catalysis.

The Asp149Asn mutant kinetics proved informative. The replacement of the charged residue by a corresponding neutral residue also results in considerably reduced activity (reduction in k_{cat} by 5×10^3) compared with wild-type PhK. To our surprise, we found that the slopes of the plots of (k^0_{cat}/k_{cat}) and $(k_{cat}/K_m)^0/(k_{cat}/K_m)$ are approximately equal to 1, indicating that the rate-limiting step was still the diffusive-dependent dissociation of the products. This step proceeds with a reduced rate constant (0.013 s^{-1}) for the Asp149Asn mutant compared with that for the native PhK (28.6 s^{-1}). There is also a significant decrease in k_2*, the on-rate for ATP to the enzyme-GPb complex, and overall there is a decrease in affinity for ATP by the Asp149Asn mutant compared with wild-type PhK (Table 4). We are only able to place a lower limit on the rate constant for the chemical step ($k_3 \geq 0.08$ s^{-1}), and we are not able to detect if the chemical step has been altered. However, we note that compared with the native PhK ($k_3 > 360$ s^{-1}), it is quite possible that the chemical step is also significantly impaired.

The effects on the ATPase activity of PhK of the mutations Asp149Ala and Asp149Asn were much less than those for the kinase activity. As shown by Paudel and Carlson (*46*), in the holoenzyme of PhK, the activation of the ATPase activity mimics the activation of the kinase activity, suggesting that the conformational changes that bring the holoenzyme into its active conformation also promote the ATPase activity. In the constitutively active PhK used in these experiments, we observe only a 4.4-fold reduction in k_{cat} for ATPase activity of the Asp149Asn mutant compared to native but with a 5×10^3 fold reduction in the kinase activity compared to native. This suggests that the role of the aspartate is more critical in the kinase reaction.

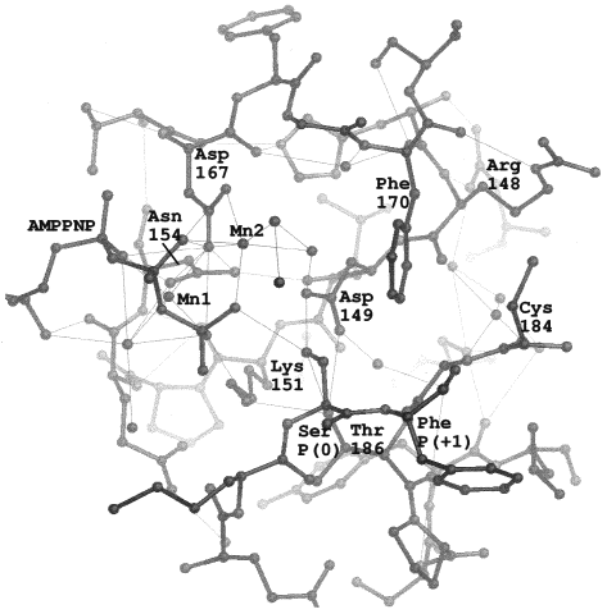

FIGURE 6: Details of the contacts between the catalytic aspartate, Asp149, and the substrates AMPPNP/Mn^{2+} and MC-peptide and surrounding residues in the ternary PhK substrate complex. One oxygen of Asp149 hydrogen bonds to Thr186, which in turn contacts Lys151. The other oxygen of Asp149 hydrogen bonds to a water molecule, that in turn contacts the metal Mn2. Asp149 also hydrogen bonds to the OG atom of the serine from the peptide substrate in its alternative conformation (see text). The serine also contacts Thr186 and the γ phosphate of AMPPNP. One metal site (Mn1) is coordinated by the terminal oxygens from the α and γ phosphates of AMPPNP, the bridging nitrogen between the β and γ phosphates, the amide oxygen of the side chain of the conserved asparagine, Asn154, from the catalytic loop, a carboxyl oxygen from the conserved Asp167 and a water molecule. The second metal site, Mn2, is coordinated by the terminal oxygens of the β and γ phosphates, two carboxyl oxygens of Asp167 and two water molecules. Diagram by OGLOBJECTS (M.E.M.N., unpublished material).

A close-up view of the residues at the catalytic site in the ternary PhK-AMPPNP-peptide substrate complex (*10*) is illustrated in Figure 6. The conserved aspartate, Asp149, is contained in the catalytic loop (in PhK residues 145−154); the loop also contains a conserved asparagine, Asn154, a residue that chelates one of the two ATP-binding metals. The aspartate, Asp149, is in a buried environment and is surrounded by the side chain of Phe170, a residue that is conserved in many but not all protein kinases. In addition, it is shielded by the peptide substrate, by residues Cys184 and Gly185 from the activation segment, and Lys151 and Asn154 from the catalytic loop. One carboxylate oxygen of Asp149 is hydrogen bonded to a water and to Thr186 which in turn is hydrogen bonded to Lys151, and the other carboxyl oxygen is hydrogen bonded to a water that in turn is chelated

to the metal Mn2. The buried nonpolar environment in a medium of low dielectric constant might argue for an increase in pK_a of the carboxyl. On the other hand, the hydrogen-bonding arrangements create a polar environment that suggests that the pK_a might be close to that observed for a carboxyl in solution, namely 4.0−4.5. Similar arguments were used to assign the likely pK_a to Asp52 in lysozyme, and the pK_a of this group was subsequently confirmed by experiment (*47*). Attempts to crystallize the Asp149Aln mutant are in progress. We note that the hydrogen-bonding arrangements for the carboxylate oxygens of Asp149 could be accommodated by the amide group of asparagine without change in structure.

The location of the triphosphate moiety of the ATP substrate is crucial for protein kinase catalysis, and in PhK, its position is defined by interactions that involve residues from both lobes of the protein kinase involving the two metal ions, the glycine loop, and two lysine residues. The contacts to the metals and Lys151 are shown in Figure 6. Contacts from the β phosphate oxygen to Ser31 and the α and β phosphate oxygens to Lys48 are out of the field of view. In the conformation of the peptide substrate seen in the ternary complex, the serine hydroxyl is 4.2 Å from the nearest carboxyl oxygen of Asp149, but within hydrogen-bonding distance to one of the γ phosphate oxygens. The position of the Ser OG atom differs from the in line position by about 45°. It has been argued (*4*, *10*) that the position of the serine may not be that taken in an active ternary complex where ATP is present rather than AMPPNP. Accordingly, the serine may be rotated from the gauche− position to the gauche+ position where it is directly in line for nucleophilic attack of the γ phosphorus. In this new position (shown in Figure 6), the OG atom is within hydrogen-bonding distance of the OD2 atom of Asp149 and a nonbridging oxygen of the γ phosphate.

The electrostatic stabilizing interactions for the triphosphate moiety of ATP involve the peripheral oxygens of the γ phosphate and not the bridging oxygen between β and γ phosphates. The nearest potential acid catalyst is Asp167 that has one of its carboxylate oxygens within 3.5 Å of the bridging oxygen. However, the angle is wrong for an approach to the lone pair electrons of the $\beta\gamma$ bridging oxygen of ATP, and both its oxygens are involved in chelating Mn1 and Mn2, making its role as a general acid catalyst unlikely.

Chemical Mechanism of Phosphoryl Transfer. The stereochemical course of phosphoryl transfer catalyzed by cAPK proceeds with inversion at the phosphorus (*48*). This rules out the possibility of a two step chemical mechanism involving, for example, the phosphorylation of an enzymic functional group such as the carboxyl group of the aspartic acid followed by phosphoryl transfer to the substrate, but is consistent with direct in-line phosphoryl transfer to the substrate hydroxyl group. The crystallographic data on PhK (*7*, *8*, *10*) and related protein kinases are consistent with the in-line mechanism of phosphoryl transfer (step 3 in the kinetic scheme in Table 2). If we accept that rotation of the serine hydroxyl group can occur from the rotamer position found in the PhK-AMPPNP-peptide complex to that which allows a strong hydrogen bond to the carboxylate ion of Asp149 when the ATP is bound, then a lone pair of electrons from the serine hydroxyl group is directed in-line to the $\beta\gamma$-bridging oxygen of the bound ATP through the γ-phosphorus atom, as depicted in Figure 6. The transition state for phosphoryl transfer by the in-line mechanism involves a pentacoordinate phosphorane in which the apical bonds are long and weak. Consequently, bond breaking of the γ-phosphoryl group from the $\beta\gamma$-bridging oxygen of ATP should be well advanced, and the bond making to the incoming nucleophile should only just be beginning at the transition state. A significant solvent isotope effect would not therefore be expected. This has been verified with cAPK using pre-steady state kinetics that allows the chemically fast phosphoryl transfer step to be investigated (*17*). Let us accept that the carboxylate ion of Asp 149 is hydrogen bonded to the serine hydroxy group in the PhK-MgATP-peptide complex. As progress along the reaction coordinate occurs, the acidity of the serine hydroxyl group will increase (i.e., it will gradually attain a lower pK_a). At the stage before phosphoryl transfer is complete, the pK_a will be below that of the carboxyl group of Asp149, and proton transfer will thus occur. Concerted proton transfer to the carboxylate ion concomitant with phosphoryl transfer is of course general base catalysis. Thus, the orientational effect and general base catalysis by the carboxyl group of Asp149 both contribute to the catalytic mechanism. This, however, leaves the carboxyl group of Asp 149 in its protonated form and so if the phosphorylated substrate were to depart, proton transfer to solvent would be the only option available. What seems more likely is that the proton is transferred to the phosphate dianion of product, simultaneously restoring the active-site carboxylate ion and allowing the now monanionic product to depart. Thus, phosphoryl transfer can be envisaged as involving both general base and general acid catalysis. In addition, there is Lys151 in close proximity to the γ phosphate of ATP, whose principal function is likely to be to stabilize the transition state and thus facilitate catalysis. It could also be responsible, in part, for binding the product ADP. These proposals are depicted schematically in Figure 7.

The proposed mechanism provides an explanation for the observed changes in the rate constants k_3 and k_4 for the Asp149Asn and Ala mutants. Thus, although one might envisage Asn fulfilling the orientation function played by Asp149, it could not function as a general base−general acid catalyst due to its inability to ionize. In the Asp149Ala mutant, the Ala could not function either as an orientational group nor as a general-acid base. It can be seen from the data in Table 4 that the mutation of Asp149 to Asn leads to a fall in the rate of substrate binding (k_2 and k_2*) and in its phosphorylation (k_3), as well as in the departure of the products (k_4). This provides powerful support for the role of the carboxylate group of Asp149, in binding and orientation of the substrate, in catalysis of phosphoryl transfer, and for the role of the negatively charged group in promoting the departure of products.

The carboxyl group of an aspartic acid residue thus appears an ideal catalytic functional group with an appropriate pK_a between a serine, threonine, or tyrosine hydroxyl group and that of the phosphorylated hydroxyl group if proton transfer did not take place. The lower flexibility of the side chain of aspartic acid compared with glutamic acid makes it a more suitable choice for its orientational role. The mechanism we propose is probably common to most if not all the protein kinases although stabilization of the transition state by the

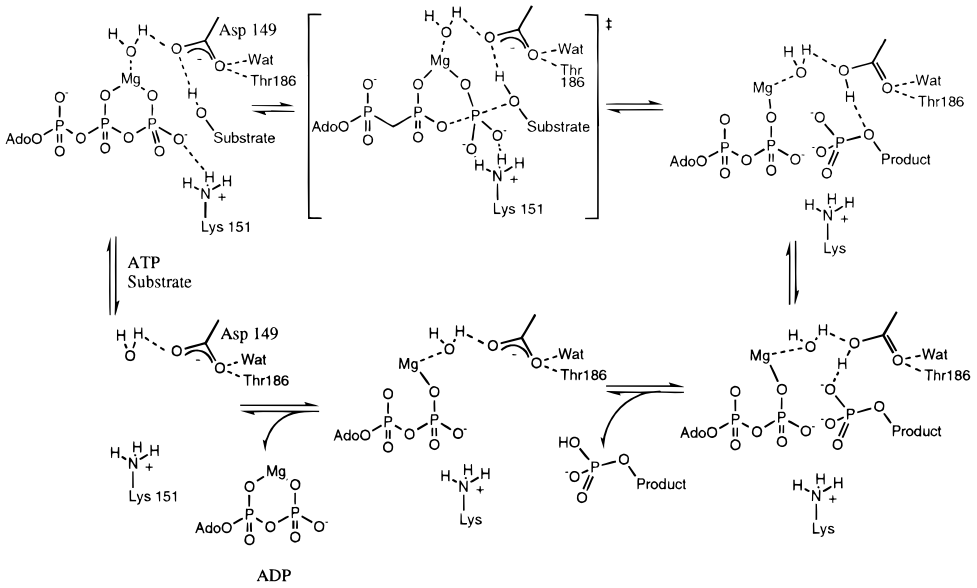

FIGURE 7: Proposals for the catalytic mechanism of PhK. Although the phosphoprotein product is shown departing before release of ADP, this order has not been established for PhK. (For further details see text.)

conjugate acid of a lysine residue may not necessarily be universal.

Role of the Activation Segment. PhK recognition of the substrate peptide is achieved through complementarity of shape, hydropathy, and electrostatic potential (*10*). The arginine residue in the peptide substrate that occupies the ($P + 2$) site has some conformational mobility in the crystal and in its best-defined position makes contact with Glu182 from the activation segment (Figure 4). The most striking aspect of the polar interactions between the peptide substrate and PhK is a short stretch of antiparallel β-sheet that is formed by main chain atoms of the peptide substrate phenylalanine in the ($P + 1$) site and the leucine in the ($P + 3$) site and residues Gly185 and Val183 from PhK. This interaction is dependent upon a defined conformation of the activation segment and implicates this region in a critical role in substrate recognition. The present kinetic results show that any perturbation of the hydrogen-bonding arrangement that locates the activation segment through contacts of Glu182, Arg148, and Tyr206 results in a decease in catalytic efficiency between 10 and 40-fold. These changes are over 12 Å from the site of catalysis. Thus, parts of the protein structure that contribute to substrate-binding site but are remote from the site of catalysis have significant contributions for turnover.

The structural result for the Glu182Ser mutant shows that change of the glutamate to a serine causes no change in the overall structure of PhK. The activation segment is held in place by a dianion that has been scavenged, most likely from the refolding β-glycerophosphate buffer, and replaces the contacts made by the glutamate to Arg148. The Glu182Ser mutant has in fact changed from being a constitutively active kinase to one that is dependent on a pseudo-phosphorylation event. The structure of the Glu182Ser mutant indicates that there is an increase in disorder of some residues of the activation segment, notably Thr186. In the peptide complex, Thr186 hydrogen bonds to Asp149, the catalytic aspartate, and to Lys151, which in turn contacts the γ phosphate of AMPPNP. This change in a crucial residue could account for the decrease in turnover seen in the kinetic studies.

The kinetic parameters for PhK activation segment mutants may be compared with those for other kinases. In cAPK, the activation segment Thr197 has been mutated to Asp and to Ala (*38*). The mutant cAPK enzymes showed a modest decease in k_{cat} by 2−14-fold and an increase of K_m for peptide and ATP. Steady-state kinetic parameters were less sensitive to viscosity than in the wild-type enzyme, and it was deduced that the chemical step (k_3) had been decreased by a factor of 10 with little change in k_4 or affinity for substrate. Similar conclusions have recently been made for the tyrosine kinase v-Fps (*49*). In both cAPK and v-Fps, phosphorylation on the residue in the activation segment is sufficient to activate. In contrast, in CDK2, both phosphorylation on Thr160 and association with cyclin are required for full activity. Phospho-CDK2 in the absence of cyclin exhibits only 0.3% of the activity observed for the fully activated complex, and X-ray crystallographic analysis of the phospho-CDK2 structure shows that the phospho-threonine by itself is insufficient to localize the activation segment (*50*). Phosphorylation results in increased disorder of the segment compared with the unphosphorylated CDK2 that may partially relieve the blocking of the ATP site observed in nonphosphorylated CDK2. Myosin I heavy-chain kinase (MIHK) is activated by phosphorylation on Ser627 in the activation segment. Szczepanowska et al. (*51*) have shown that mutation of Ser627 to Ala, Asp, and Glu resulted in mutants that were less active than wild type with reduction in k_{cat} by 7, 9, and 2-fold, respectively, and increases in K_m for peptide and ATP of the order of 5−8- and 3−5-fold. Interestingly, the Ser627Glu mutant was the most active of the mutants, indicating that the charged group was able to partially compensate for the phospho-serine but was unable to produce full activity. Mutation of Thr631 in MIHK (the residue that corresponds to Thr186 in PhK) to Ala resulted in a 3-fold reduction in k_{cat} and a 10- and 7-fold increase in K_m for peptide and ATP, indicating a role for this conserved threonine in catalysis, as suggested from the structural and present kinetic studies on PhK. In v-src, mutation of Arg385 (equivalent to Arg148 in PhK) to Ala had significant effects on kinase activity (*52*). Rates were reduced by 10-fold with

respect to wild-type Src and by 190-fold with respect to the mutant Tyr527Phe Src in ability to phosphorylate exogenous substrates. When introduced into an activated *v-src* gene, Arg385Ala totally blocked cell transformation.

Taken together, these results indicate the importance of the activation segment localization in catalysis. However, changes in turnover rates on mutation of residues in the activation segment are considerably less than the reduction in rates observed on mutation of the catalytic aspartate. Comparison of active and inactive kinase structures solved to date show that there is little change in the position of the catalytic aspartate on activation. The activation process results in changes in the protein components that recognize the ATP and protein substrates. The structural changes allow the correct presentation and orientation of the substrates with respect to each other and to the aspartate. In view of the fact that mutation of residues in the activation segment may result in small but not totally deleterious changes in kinetic parameters, it is surprising that phosphorylation of residues in the activation segment is used so ubiquitously as a control mechanism for protein kinases. In many kinases where it is crucial for the kinase to remain inactive until activated by signaling, there are other control mechanisms that involve phosphorylation at other sites or association with other subunits.

ACKNOWLEDGMENT

We wish to acknowledge Steven Dyson for early work on the expression of the Glu182Ser mutant. We are grateful to the staff at beam line ID3, ESRF, Grenoble for their help with the use of the beamline. Finally, we thank Richard Bryan and Yuguang Huang for support for computing.

REFERENCES

1. The *C. elegans* Sequencing Consortium. (1998) *Science 282*, 2012−2018.
2. Hunter, T. (1987) *Cell 50*, 823−825.
3. Hanks, S. K., and Hunter, T. (1995) *FASEB J. 9*, 576−596.
4. Johnson, L. N., Lowe, E. D., Noble, M. E. M., and Owen, D. J. (1998) *FEBS Lett. 430*, 1−11.
5. Fischer, E. H., and Krebs, E. G. (1955) *J. Biol. Chem. 216*, 121−132.
6. Pickett-Gies, C. A., and Walsh, D. A. (1986) in *The Enzymes* (Boyer, P. D., and Krebs, E. G., Eds.) pp 396−459, Academic Press, Orlando, Florida.
7. Owen, D. J., Papageorgiou, A. C., Garman, E. F., Noble, M. E. M., and Johnson, L. N. (1995) *J. Mol. Biol. 246*, 376−383.
8. Owen, D. J., Noble, M. E., Garman, E. F., Papageorgiou, A. C., and Johnson, L. N. (1995) *Structure 3*, 467−482.
9. Graves, D. J. (1983) *Methods Enzymol. 99*, 268−278.
10. Lowe, E. D., Noble, M. E. M., Skamnaki, V. T., Oikonomakos, N. G., Owen, D. J., and Johnson, L. N. (1997) *EMBO J. 16*, 6646−6658.
11. Valon, C., Smalle, J., Goodman, H. M., and Giraudat, J. (1993) *Plant Mol. Biol. 23*, 415−421.
12. Bossmeyer, D., Engh, R. A., Kinzel, V., Ponstingl, H., and Huber, R. (1993) *EMBO J. 12*, 849−859.
13. Zheng, J., Trafny, E. A., Knighton, D. R., Xuong, N., Taylor, S. S., Eyck, L. F. T., and Sowadski, J. M. (1993) *Acta Crystallogr., Sect. D 49*, 362−365.
14. Madhusudan, Trafny, E. F., Xuong, N., Adams, J. A., Eyck, L. F. T., Taylor, S. S., and Sowadski, J. M. (1994) *Protein Sci. 3*, 176−187.
15. Hubbard, S. R. (1997) *EMBO J. 16*, 5572−5581.
16. Yoon, M.-Y., and Cook, P. F. (1987) *Biochemistry 26*, 4118−4125.
17. Zhou, J., and Adams, J. A. (1997) *Biochemistry 36*, 2977−2984.
18. Cole, P. A., Grace, M. R., Phillips, R. S., Burn, P., and Walsh, C. T. (1995) *J. Biol. Chem. 270*, 22105−22108.
19. Adams, J. A., and Taylor, S. S. (1992) *Biochemistry 31*, 8516−8522.
20. Whitehouse, S., Feramisco, J. R., Casnellie, J. E., Krebs, E. G., and Walsh, D. A. (1983) *J. Biol. Chem. 258*, 3693−3701.
21. Adams, J. A., and Taylor, S. S. (1993) *J. Biol. Chem. 268*, 7747−7752.
22. Johnson, L. N., Noble, M. E. M., and Owen, D. J. (1996) *Cell 85*, 149−158.
23. Knighton, D. R., Zheng, J., Ten Eyck, L. F., Ashford, V. A., Xuong, N.-H., Taylor, S. S., and Sowadski, J. M. (1991) *Science 253*, 407−413.
24. Russo, A., Jeffrey, P. D., and Pavletich, N. P. (1996) *Nat. Struct. Biol. 3*, 696−700.
25. Canagarajah, B. J., Khokhlatchev, A., Cobb, M. H., and Goldsmith, E. J. (1997) *Cell 90*, 859−869.
26. Yamaguchi, H., and Hendrickson, W. A. (1996) *Nature 384*, 484−489.
27. Mayans, O., van der veen, P. F. M., Wilm, M., Mues, A., Young, P., Furst, D. O., Willmanns, M., and Gautel, M. (1998) *Nature 395*, 863−869.
28. Way, M., Pope, B., Goode, J., Hawkins, M., and Weeds, A. G. (1990) *EMBO J. 9*, 4103−4109.
29. Helmreich, E. J. M., and Cori, C. F. (1964) *Proc. Natl. Acad. Sci. U.S.A. 51*, 131−138.
30. Melpidou, A. E., and Oikonomakos, N. G. (1983) *FEBS Lett. 154*, 105−110.
31. Kastenscmidt, L. L., Kastenschmidt, J., and Helmreich, E. J. M. (1968) *Biochemistry 7*, 3590−3608.
32. Bradford, M. M. (1976) *Anal. Biochem. 72*, 248−254.
33. Cohen, P. (1983) *Methods Enzymol. 99*, 243−259.
34. Uyttenhove, K., Bollen, M., and Stallmans, W. (1991) *Biochem. J. 278*, 899−904.
35. Oikonomakos, N. G., Zographos, S. E., Johnson, L. N., Papageorgiou, A. C., and Acharya, K. R. (1995) *J. Mol. Biol. 254*, 900−917.
36. Leatherbarrow, R. J. (1992) *GrafFit Version 3.0*, Erithakus Software, Staines, U.K.
37. Cook, F. N., Neville, M. E., Vrana, K. E., Hartl, F. T., and Roskowski, R. (1982) *Biochemistry 21*, 5794−5799.
38. Adams, J. A., McGlone, M. L., Gibson, R., and Taylor, S. S. (1995) *Biochemistry 34*, 2447−2454.
39. Jones, T. A., Zou, J. Y., Cowan, S. W., and Kjeldgaard, M. (1991) *Acta Crystallogr., Sect. A 47*, 110−119.
40. Murshudov, G. N., Vagen, A. A., and Dodson, E. J. (1997) *Acta Crystallogr., Sect. D 53*, 240−255.
41. Grant, B. D., and Adams, J. A. (1996) *Biochemistry 35*, 2022−2029.
42. Tabatabai, L. B., and Graves, D. J. (1978) *J. Biol. Chem. 253*, 2196−2202.
43. Read, R. J. (1986) *Acta Crystallogr., Sect. A 42*, 140−149.
44. Cox, S., and Johnson, L. N. (1992) *Protein Eng. 5*, 811−819.
45. Gibbs, C. S., Knighton, D. R., Sodwadski, J. M., Taylor, S. S., and Zoller, M. J. (1992) *J. Biol. Chem. 267*, 4806−4814.
46. Paudel, H. K., and Carlson, G. M. (1991) *J. Biol. Chem. 266*, 16524−16529.
47. Imoto, T., Johnson, L. N., North, A. C. T., Phillips, D. C., and Rupley, J. A. (1972) in *The Enzymes* (Boyer, B., Ed.) Academic Press, New York.
48. Ho, M. F., Bramson, H. N., Hansen, D. E., Knowles, J. R., and Kaiser, E. T. (1988) *J. Am. Chem. Soc. 110*, 2680−2681.
49. Saylor, P., Hanna, E., and Adams, J. A. (1998) *Biochemistry 37*, 17875−17881.
50. Brown, N. R., Noble, M. E. M., Lawrie, A. M., Morris, M. C., Tunnah, P., Divita, G., N., J. L., and Endicott, J. A. (1999) *J. Biol. Chem. 274*, 8746−8756.
51. Szczepanowska, J., Ramachandran, U., Herring, C. J., Gruschus, J. M., Qin, J., Korn, E. D., and Brzeska, H. (1998) *Proc. Natl. Acad. Sci. U.S.A. 95*, 4146−4151.
52. Senften, M., Schenker, G., Sowadski, J. M., and Ballmer-Hofer, K. (1995) *Oncogene 10*, 199−203.

BI991454F